Protist, Vol. 170, 38–51, February 2019
http://www.elsevier.de/protis
Published online date 24 October 2018

Protist

ORIGINAL PAPER

Non-linear Physiology and Gene Expression Responses of Harmful Alga *Heterosigma akashiwo* to Rising CO_2

Gwenn M.M. Hennon[a], Olivia M. Williamson[b,2], María D. Hernández Limón[c], Sheean T. Haley[a], and Sonya T. Dyhrman[a,d,1]

[a]Department of Biology and Paleo Environment, Lamont-Doherty Earth Observatory, Palisades, NY, USA
[b]Barnard College, New York, NY, USA
[c]Columbia University, New York, NY, USA
[d]Department of Earth and Environmental Sciences, Columbia University, New York, NY, USA

Submitted June 6, 2018; Accepted October 15, 2018
Monitoring Editor: Chris Bowler

Heterosigma akashiwo **is a raphidophyte known for forming ichthyotoxic blooms. In order to predict the potential impacts of rising CO_2 on *H. akashiwo* it is necessary to understand the factors influencing growth rates over a range of CO_2 concentrations. Here we examined the physiology and gene expression response of *H. akashiwo* to concentrations from 200 to 1000 ppm CO_2. Growth rate data were combined from this and previous studies and fit with a CO_2 limitation-inhibition model that revealed an apparent growth optimum around 600–800 ppm CO_2. Physiological changes included a significant increase in C:N ratio at ~800 ppm CO_2 and a significant decrease in hydrogen peroxide concentration at ~1000 ppm. Whole transcriptome sequencing of *H. akashiwo* revealed sharp distinctions in metabolic pathway gene expression between ~600 and ~800 ppm CO_2. Hierarchical clustering by co-expression identified groups of genes with significant correlations to CO_2 and growth rate. Genes with significant differential expression with CO_2 included carbon concentrating mechanism genes such as beta-carbonic anhydrases and a bicarbonate transporter, which may underpin shifts in physiology. Genes involved in cell motility were significantly changed by both elevated CO_2 and growth rate, suggesting that future ocean conditions could modify swimming behavior in this species.**

© 2018 Elsevier GmbH. All rights reserved.

Key words: Ichthyotoxic; harmful algal bloom; carbon concentrating mechanism; raphidophyte; climate change; ocean acidification.

Introduction

Over the last century anthropogenic emissions of CO_2 have resulted in rising atmospheric CO_2 and the carbonation and acidification of the global oceans (Ciais et al. 2013; Sabine et al. 2004). The increase in dissolved CO_2 and concomitant

[1]Corresponding author;
[2]Present address: Department of Marine Biology & Ecology, Rosenstiel School of Marine & Atmospheric Science, University of Miami, Miami, FL, USA.
e-mail sdyhrman@ldeo.columbia.edu (S.T. Dyhrman).

https://doi.org/10.1016/j.protis.2018.10.002
1434-4610/© 2018 Elsevier GmbH. All rights reserved.

decrease in ocean pH are projected to continue over the present century (Caldeira and Wickett 2003; Ciais et al. 2013), resulting in significant impacts on marine organisms (Brierley and Kingsford 2009; Doney et al. 2009). A global marine ecosystem model that integrated the various responses of phytoplankton groups to rising CO_2 predicted significant shifts in species dominance under future CO_2 conditions (Dutkiewicz et al. 2015). These community shifts may exacerbate an already difficult and persistent problem for coastal and estuarine communities, the prediction of harmful algal blooms (HAB) (Hallegraeff 2010). HABs are increasing worldwide (Anderson et al. 2012; Hallegraeff 1993), reported in locations and seasons in which they have never been detected before (Daley 2018). A modeling study focused on two dinoflagellate HAB species predicted a northern range and seasonal expansion of toxic blooms with rising temperatures in the North Atlantic and Pacific (Gobler et al. 2017). To date, several studies have reported that HAB species, particularly dinoflagellates and raphidophytes, have enhanced growth rates with ocean acidification predicted for 2100 (Fu et al. 2008; Ou et al. 2017; Pang et al. 2017), suggesting that rising CO_2 could also promote HAB events.

The marine raphidophyte, *Heterosigma akashiwo*, is a widely distributed coastal and estuarine species capable of forming HABs (Honjo 1992). *H. akashiwo* blooms have been reported to be ichthyotoxic, causing mortality events in both farmed and wild fish populations (Itakura and Imai 2014; Rensel et al. 2010;Taylor and Haigh 1993). Despite strain-to-strain differences, it is well-reported that *H. akashiwo* tolerates a wide range of environmental variables, including light (Butrón et al. 2012), salinity (Strom et al. 2013), and temperature (Zhang et al. 2006). *H. akashiwo* growth rates have been shown to significantly increase under elevated CO_2 and acidification predicted for the year 2100 (Fu et al. 2008; Hennon et al. 2017). Swimming behavior has been reported to be impacted by shifts in pH, implying that *H. akashiwo* has the ability to sense and respond to changes in carbonate chemistry (Kim et al. 2013). In fact, CO_2-stimulated growth rate enhancement gave *H. akashiwo* an advantage in co-culture experiments with the non-toxic diatom *Skeletonema costatum* (Xu et al. 2010), suggesting that under future CO_2 conditions HABs of *H. akashiwo* may increase in frequency and severity by outcompeting other coastal phytoplankton species.

The cause of growth rate enhancement under elevated CO_2 is not definitively known for *H. akashiwo*, but physiological evidence suggests that raphidophytes may be carbon-limited in the modern ocean. Nimer et al. (1997) found that raphidophytes did not take up external bicarbonate or extracellularly convert bicarbonate to CO_2, making them one of the few marine phytoplankton groups to apparently lack a way to use bicarbonate from their environment. In another study, *H. akashiwo* had a higher rate of beta-carboxylation relative to Rubisco carboxylation (Descolas-Gros and Oriol 1992), suggesting that carbon fixation by Rubisco is very slow in raphidophytes and may be compensated for by more energetically expensive carbon fixation pathways. These studies suggest that *H. akashiwo* relies on CO_2 diffusion to supply carbon to Rubisco, hence elevated CO_2 allows for an increased rate of carbon fixation. However, with the first transcriptomes for *H. akashiwo* and other raphidophytes now available (Haley et al. 2017; Keeling et al. 2014), genes with homology to bicarbonate transporters, carbonic anhydrases as well as C3 and C4 pathway genes were identified in these assembled transcriptomes (Hennon et al. 2017). Carbonic anhydrase genes were found to shift expression in concert with carbon fixation genes in both lab and field studies of *H. akashiwo* (Hennon et al. 2017; Ji et al. 2018). These recent findings suggest that at least some raphidophytes may in fact have the genetic capacity to use bicarbonate with a carbon (or CO_2) concentrating mechanism (CCM).

The physiological responses, and their genetic underpinnings, to a broad range of CO_2 conditions are largely unknown for toxic *H. akashiwo* strain CCMP2393. Here we measured physiological changes of *H. akashiwo* in response to CO_2 conditions ranging from pre-industrial (~200 ppm) to those predicted for year 2100 (~1000 ppm) (Ciais et al. 2013). We complemented physiological measurements with whole transcriptome sequencing to not only assess genetic capabilities but also to identify and compare mechanistic shifts along the CO_2 gradient.

Results and Discussion

Changes in growth rates, physiology, and gene expression in *H. akashiwo* were measured in response to a range of CO_2 concentrations in order to examine potential non-linear responses over a variety of predicted CO_2 concentration scenarios. The highest mean growth rate for *H. akashiwo*

Table 1. Physiology of *H. akashiwo* under a range of CO_2 scenarios. CO_2 scenarios include pre-modern, modern and three representative concentration pathways (RCP) (Ciais and Sabine 2013). Mean values ± standard deviation for CO_2 concentration (ppm), growth rate (day^{-1}), carbon per cell (pg C $cell^{-1}$), nitrogen per cell (pg N $cell^{-1}$), and chlorophyll concentration (pg $cell^{-1}$).

	200 (premodern)	400 (modern)	600 (RCP4.5)	800 (RCP6.0)	1000 (RCP8.5)
CO_2 (ppm)	265 ± 45	423 ± 51	571 ± 74	780 ± 80	1017 ± 98
Growth rate (day^{-1})	0.61 ± 0.09	0.63 ± 0.04	0.70 ± 0.11	0.77 ± 0.12	0.54 ± 0.13
Carbon (pg $cell^{-1}$)	240 ± 82	219 ± 50	151 ± 8	226 ± 31	181 ± 13
Nitrogen (pg $cell^{-1}$)	57 ± 18	50 ± 11	37 ± 2	44 ± 8	41 ± 5
Chlorophyll *a* (pg $cell^{-1}$)	0.74 ± 0.12	0.52 ± 0.26	0.31 ± 0.13	0.43 ± 0.02	0.45 ± 0.08

(0.77 d^{-1}) was measured for cultures maintained at ~800 ppm CO_2. However, there was no significant difference in growth rates among the CO_2 treatments in this study due to high variability in the biological replicates (Table 1, ANOVA $p > 0.05$). Despite this variability, the range of growth rates was remarkably consistent with previous studies. A comparison of growth rate responses of *H. akashiwo* from this study with those from the literature (Fig. 1) showed that, despite the differences in culturing conditions between labs, and strain variability, the growth rate responses were similar for *H. akashiwo* under the same concentrations of CO_2 (Fig. 1). In contrast to previous studies, our study examined a greater number of CO_2 treatments spanning pre-industrial (~200 ppm) to the business-as-usual scenario predicted for 2100 (~1000 ppm) (Supplemental Material Table S1). When the growth rate data from all available studies are considered together, there is an apparent maximum in growth rates around 700 ppm, and a decline in growth rate at CO_2 greater than 800 ppm (Fig. 1). Growth rate data were fit with a CO_2 limitation-inhibition model (See Methods: Equation (1)) that predicted a half-saturation of 236 ± 114 ppm CO_2 with a maximum theoretical growth rate of 3.0 ± 0.7 day^{-1} and an inhibition coefficient of 0.0006 ± 0.0002 ppm^{-1} CO_2.

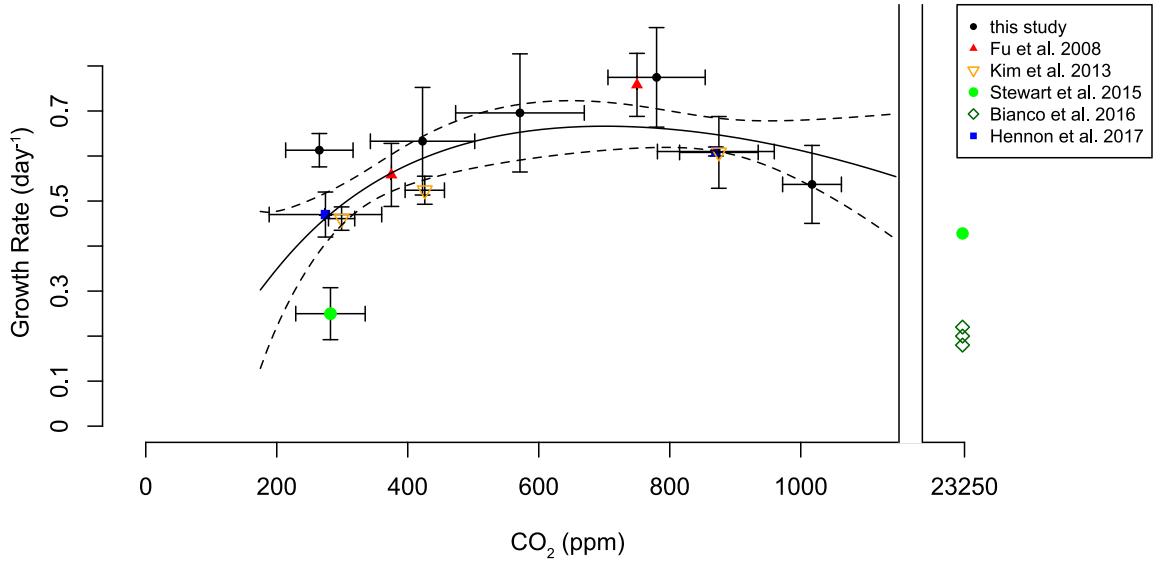

Figure 1. Growth rate response of *Heterosigma akashiwo* for a range of CO_2 concentrations. Exponential growth rate (day^{-1}, mean ± SD) versus CO_2 concentration (μatm, mean ± SD) for *H. akashiwo* compiled from the literature and in this study. Black circles indicate data from this study (n = 3), red squares: from Fu et al. 2008 (n = 3), orange triangles: Kim et al. 2013 (n = 3), green circles: Stewart et al. 2015 (n = 4), green diamonds: Bianco et al. 2016 (n = 4), and blue squares: Hennon et al. 2017 (n = 3). Solid line indicates the mean best fit for a CO_2 limitation-inhibition model with dashed lines to indicate one standard deviation of the model fit with the Monte Carlo method (1000 simulations).

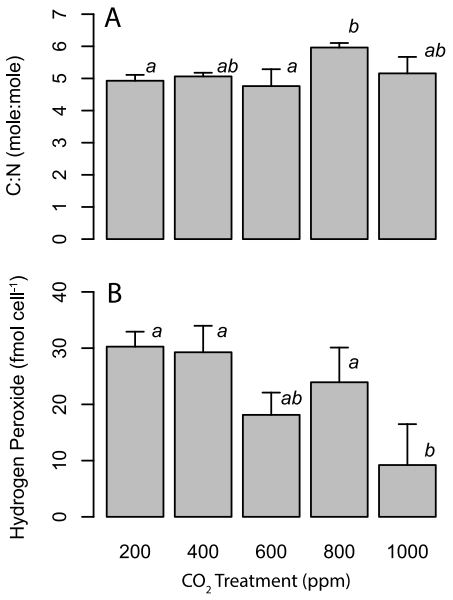

Figure 2. Physiological response of *Heterosigma akashiwo* to a range of CO_2 treatments. Bar plots of (**A**) carbon to nitrogen ratio (C:N), and (**B**) hydrogen peroxide (fmol cell^{-1}) with mean and standard deviation indicated by error bar (n = 3). Letters above bars indicate significant differences from ANOVA ($p < 0.05$) and post hoc Tukey HSD test ($p < 0.05$).

Estuarine waters where *H. akashiwo* thrives often have lower pH and higher pCO_2 than the open ocean as a consequence of upwelling of deep water (Feely et al. 2010), potentially explaining why the apparent growth optimum is at a CO_2 concentration greater than modern atmospheric concentrations.

Physiological measurements of *H. akashiwo* over the range of CO_2 treatments revealed a trend of declining chlorophyll *a* concentrations at higher CO_2 similar to previous studies (Hennon et al. 2017), although the differences were not statistically significant (Table 1), perhaps due to the loss of one of the biological replicate samples. Significant differences in carbon to nitrogen ratio (C:N) and hydrogen peroxide concentration per cell (Fig. 2A) were also observed. The significant increase in C:N ratio at 800 ppm CO_2 and the apparent decline in chlorophyll *a* content per cell correspond well to a previously measured increase in carbohydrate production and decrease in chlorophyll *a* in *H. akashiwo* under elevated CO_2 (Hennon et al. 2017). Previous studies have found increased C:N ratio in the elevated CO_2 treatments of community mesocosm experiments (Riebesell et al. 2007), suggesting this could be a general phytoplankton response with potential to increase the efficiency of carbon export and decrease the quality of phytoplankton as food for higher trophic levels. The significant decrease in hydrogen peroxide concentration at 1000 ppm CO_2 (Fig. 2B) could derive from either a decrease in hydrogen peroxide production or an increase in degradation rates. Raphidophytes have been reported to have relatively high rates of hydrogen peroxide and superoxide production (Dorantes-Aranda et al. 2015; Twiner and Trick 2000). While this is likely not the main cause of ichthyotoxicity in *H. akashiwo* (Twiner et al. 2001), free radical concentrations can serve as an indicator of metabolic activity, and potential oxidative stress (Twiner and Trick 2000). In order to predict the impact of these physiological changes on ecological success, it is necessary to identify which metabolic pathways were differentially expressed.

Whole transcriptome sequencing was performed on biological triplicate bottles of *H. akashiwo* cultures acclimated to five concentrations of CO_2 from 200 to 1000 ppm to examine the genetic mechanisms of the response to CO_2 for this species. The cultures were non-axenic, so polyA selection was used to capture only the eukaryotic RNA. To get a broad view of metabolic changes, RNA reads were aligned to the *H. akashiwo* contigs and groups of genes belonging to KEGG pathways were filtered for significant changes in expression distribution (Kolmogorov-Smirnov test, $p < 0.05$) among CO_2 treatments compared with 400 ppm CO_2 (Fig. 3). Metabolic pathways involved in the same processes displayed similar patterns of expression across CO_2 treatments (Fig. 3). For example, light gathering pathways of photosynthesis and biosynthesis pathways for chlorophyll and other photosynthetic pigments grouped together and had decreased expression at both pre-industrial (200 ppm) and elevated CO_2 (800–1000 ppm) treatments compared to ambient (400 ppm) CO_2 (Fig. 3). Likewise, other core carbon metabolic pathways like glycolysis and C3 carbon fixation had decreased expression at elevated CO_2 (800–1000 ppm) despite no significant change in growth rates (Fig. 3). This observation is similar to the decrease in core metabolic gene expression observed in the diatom, *Thalassiosira pseudonana*, under elevated CO_2 (Hennon et al. 2015) with no change in growth rate, thought to be a response to down-regulation of CCM genes. Genes involved in cell cycle, DNA replication, and DNA repair grouped together with a pattern of increased expression at elevated (800–1000 ppm) CO_2 (Fig. 3). These results suggest there may be increased damage as well as replication of genomic DNA. A peroxidase gene was also significantly differentially expressed with elevated expression

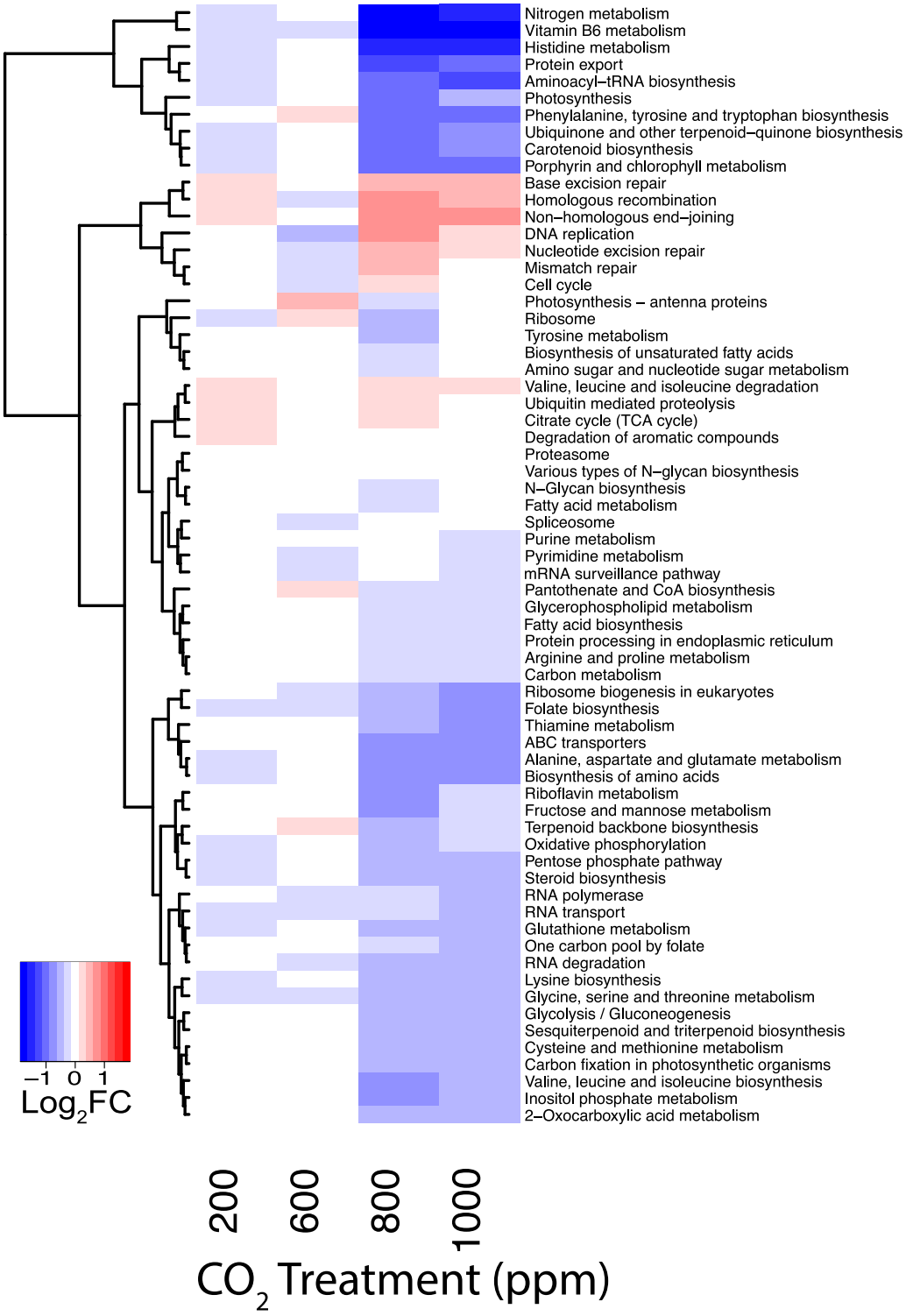

Figure 3. Changes in KEGG pathway expression of *Heterosigma akashiwo* under a range of CO_2 treatments. Heatmap colors indicate the mean $\log_2$ (fold change) in expression of genes in each KEGG pathway according to the color bar for each CO_2 treatment relative to 400 ppm, with red indicating increased expression, blue indicating decreased expression and white indicating no change in expression. The dendrogram indicates similarity in KEGG pathway expression. All KEGG pathways shown have a significantly different distribution relative to 400 ppm in at least one of the treatments (Kolmogorov–Smirnov test $p < 0.05$).

at 800–1000 ppm (CAMPEP_0188594904, Supplementary Material Table S2). The decreased concentration of hydrogen peroxide (Fig. 2) could potentially be explained by an increase in expression of a peroxidase enzyme at elevated CO_2.

The most striking change in KEGG pathway expression was for nitrogen metabolism genes with a greater than 2-fold decrease at elevated (800–1000 ppm) CO_2 (Fig. 3). The decreased nitrogen metabolism gene expression may underpin the increased C:N ratio at 800 ppm, yet upon inspection, this expression pattern is largely driven by a few carbonic anhydrase genes that are potentially involved in either nitrogen pathways or CCMs. Differential expression analysis across CO_2 treatments revealed significant differences in the transcript levels of 121 genes (exact test, false discovery rate <0.05, Supplementary Material Table S2). To determine whether the patterns of CCM gene expression were more closely related to CO_2 treatment or changes in growth physiology, the putative CCM genes were tested for a significant monotonic increase or decrease in expression (Pearson correlation) with CO_2 or growth rate. This analysis took advantage of the wide range in CO_2 concentrations and growth rates measured in this study, using data for each individual biological replicate sample rather than grouping samples by treatment. Putative CCM genes including all contigs with significant homology to alpha and beta carbonic anhydrases, bestrophins and bicarbonate transporters are listed in Table 2 along with their putative locations in the cell. A select few putative CCM genes had both significant differences in expression by CO_2 treatment and a monotonic decrease with CO_2 (beta CA-4,5,9 and SLC4-2: Table 2) as would be expected for a CO_2-responsive CCM. Two of three CO_2-responsive carbonic anhydrases had a predicted localization to the plastid, suggesting they operate in close proximity to Rubisco (beta-CA4 and beta-CA5, Table 2). SLC4-2 is a putative bicarbonate transporter, which displayed lower expression under both 800 and 1000 ppm CO_2 relative to 400 ppm CO_2. SLC4 bicarbonate transporters have been shown to transport bicarbonate from the seawater media into diatoms (Nakajima et al. 2013) as part of the CCM. These results support a CO_2-responsive biophysical CCM in this raphidophyte and suggest that selected plastid-targeted beta-CAs and an external bicarbonate transporter are the key genes controlling the response of *H. akashiwo* to changing CO_2 conditions, similar to those described for the well-characterized diatom, *Phaeodactylum tricornutum* (Harada et al. 2006; Nakajima et al. 2013).

Hierarchical clustering revealed co-expression relationships between genes and correlations to either CO_2 or growth rate (Fig. 4). A cluster of genes involved in flagellar motion and motility were found to be positively correlated with CO_2 (Pearson correlation = 0.56, p-value = 0.03, Fig. 4A), while a separate cluster of motility genes was significantly correlated to growth rate (Pearson correlation = 0.66, p-value <0.01, Fig. 4E). The increased expression of motility genes with increased CO_2 is consistent with observations from a previous study that found enhanced downward swimming behavior of *H. akashiwo* under elevated CO_2 (Kim et al. 2013). Although swimming behavior was not measured in this study, the gene expression patterns suggest that both elevated CO_2 and growth rate were correlated with enhanced expression of motility genes (Fig. 4A,E). A Ras-family signaling pathway gene was significantly differentially expressed with respect to CO_2 treatment (contig ID: 13233_1, Supplementary Material Table S2) and falls within the CO_2-responsive motility gene cluster (Fig. 4A: cluster 143). Although Ras-family signaling genes can impact many possible cell functions, the co-expression of these genes suggests that this particular Ras signaling pathway gene may be involved in the regulation of motility genes in *H. akashiwo* that are influenced by CO_2. Swimming behavior in *H. akashiwo* is an important facet of bloom ecology, as the raphidophyte can form or disaggregate surface slicks due to coordinated swimming (Bearon et al. 2004). Down-swimming in response to elevated CO_2 as observed by Kim et al. (2013) could serve to disaggregate surface blooms and possibly decrease encounters with surface predators. The expression response in motility genes identified herein may underpin changes in swimming behavior and offers an avenue for further study of this aspect of bloom dynamics in the future ocean.

The CO_2-responsive CCM genes were grouped into three clusters (Fig. 4B,C,D) with 38, 386 and 401 genes, respectively. The beta-CA4 gene was part of the 38-gene cluster (Fig. 4B, cluster 174) that was significantly anti-correlated with CO_2 (pearson correlation = −0.70, p-value <0.01, Supplementary Material Tables S3 and S4). Other genes in the cluster included a sodium/proton antiporter (Na^+/H^+ antiporter, Fig. 4B) and potential regulatory genes with dnaJ and RNA-binding domains (Supplementary Material Table S3). The Na^+/H^+ antiporter could be involved in pH homeostasis or in the functioning of a *H. akashiwo* CCM. The maintenance of an acidified thylakoid compartment within the plastid may be important for an efficient biophysical CCM

Table 2. Putative biophysical CCM genes from *H. akashiwo* with summary statistics and predicted localization. Gene names are assigned according to homology with alpha or beta carbonic anhydrases (CA), bestrophins (Best) and SLC4 bicarbonate transporters (SLC4). For clarity, gene names have been abbreviated and amended with numbers to indicate unique genes. Summary statistics include: exact test (edgeR) to test for differences among CO_2 treatments, and pearson correlation tests to determine whether genes display a significant monotonic change with CO_2 or growth rate. The predicted localization of genes products was determined by SignalP and ASAFind.

Gene Name	Peptide ID	exact test (fdr)	pearson CO_2	pearson growth rate	localization
alpha-CA1	CAMPEP_0188570690	0.27	−0.44	0.07	Not plastid, SignalP negative
alpha-CA2	CAMPEP_0188571210	0.33	−0.30	0.04	Plastid, high confidence
alpha-CA3	CAMPEP_0188570788	0.37	−0.42	0.06	Plastid, low confidence
alpha-CA4	CAMPEP_0188575582	0.51	−0.41	0.03	Plastid, low confidence
alpha-CA5	CAMPEP_0188582928	0.43	−0.43	0.03	Not plastid, SignalP negative
alpha-CA6	CAMPEP_0188565536	not expressed			Not plastid, SignalP negative
alpha-CA7	CAMPEP_0188572346	0.32	−0.49	0.05	Not plastid, SignalP negative
alpha-CA8	CAMPEP_0188580680	0.51	−0.44	0.18	Not plastid, SignalP negative
alpha-CA9	CAMPEP_0188589552	1.00	0.11	−0.59	Not plastid, SignalP negative
alpha-CA10	CAMPEP_0188555996	1.00	−0.09	0.50	Plastid, low confidence
beta-CA1	CAMPEP_0188570370	1.00	−0.46	0.17	Not plastid, SignalP negative
beta-CA2	CAMPEP_0188569706	1.00	0.59	−0.08	Not plastid, SignalP negative
beta-CA3	CAMPEP_0188590882	0.66	−0.47	0.06	Plastid, high confidence
beta-CA4	CAMPEP_0188557288	0.00	−0.88	0.04	Plastid, high confidence
beta-CA5	CAMPEP_0188571404	0.00	−0.79	0.06	Plastid, high confidence
beta-CA6	CAMPEP_0188597438	0.76	−0.40	−0.07	Not plastid, SignalP negative
beta-CA7	CAMPEP_0188571148	0.98	−0.36	−0.11	Plastid, high confidence
beta-CA8	CAMPEP_0188575444	0.91	−0.46	0.04	Plastid, high confidence
beta-CA9	CAMPEP_0188586576	0.02	−0.75	0.09	Not plastid, SignalP negative
beta-CA10	CAMPEP_0188590874	0.55	−0.45	0.07	Not plastid, SignalP negative
Best-1	CAMPEP_0188596298	0.59	−0.50	0.01	Plastid, high confidence
Best-2	CAMPEP_0188569350	0.53	−0.45	0.06	Plastid, high confidence
Best-3	CAMPEP_0188546542	0.47	−0.48	0.11	Plastid, high confidence
Best-4	CAMPEP_0188597218	0.13	−0.54	0.19	Plastid, high confidence
Best-5	CAMPEP_0188597062	1.00	0.00	0.20	Not plastid, SignalP negative
Best-6	CAMPEP_0188567114	0.39	−0.47	0.23	Not plastid, SignalP positive
SLC4-1	CAMPEP_0188568326	1.00	−0.18	−0.04	Not plastid, SignalP negative
SLC4-2	CAMPEP_0188598466	0.03	−0.41	0.21	Not plastid, SignalP negative
SLC4-3	CAMPEP_0188555726	1.00	−0.36	0.13	Not plastid, SignalP negative

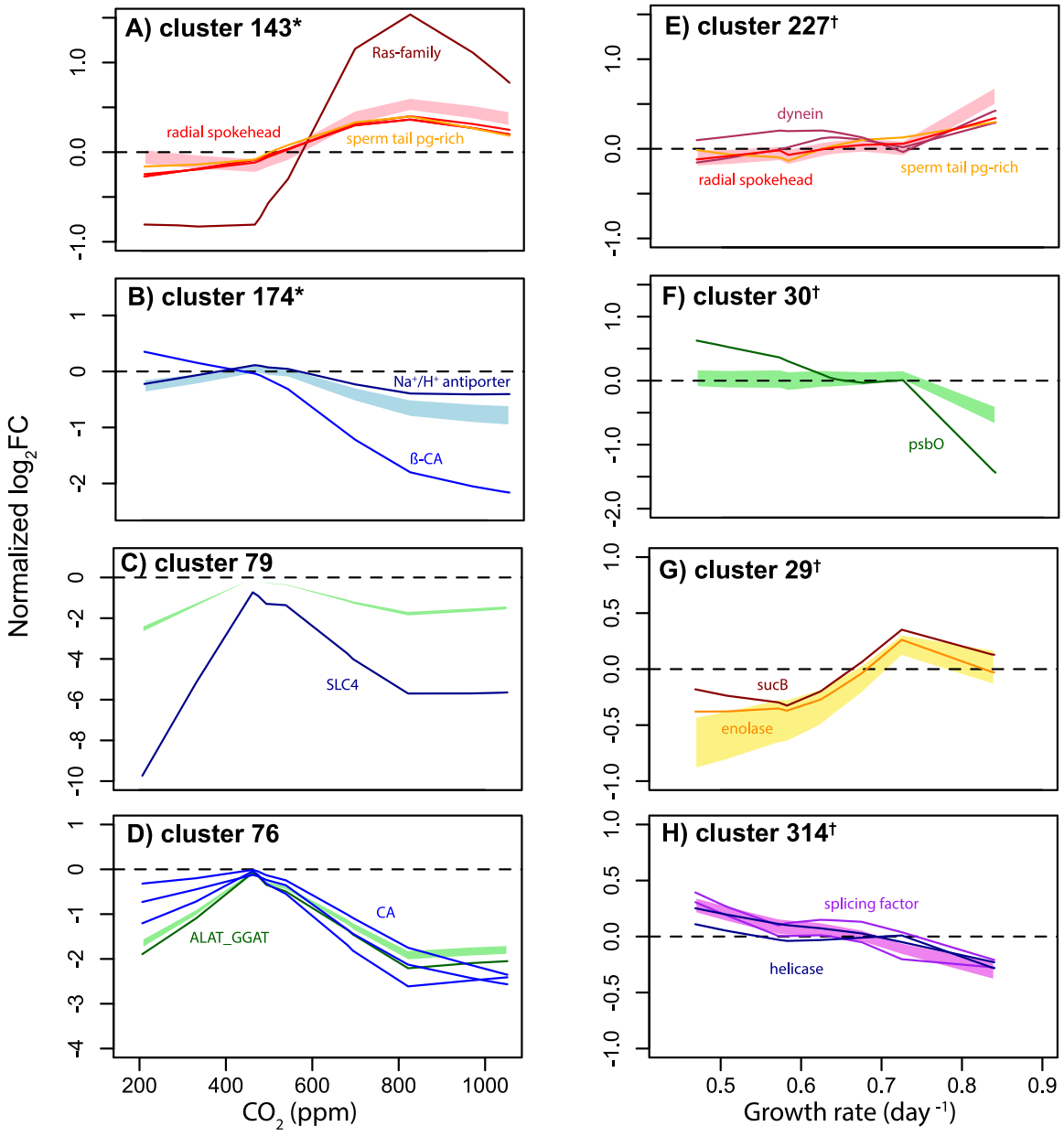

Figure 4. Co-expressed gene clusters correlated with growth rate and CO_2. The log transformed fold change (log_2 FC) of transcript abundance relative to modern CO_2 treatments of selected genes and gene clusters from *H. akashiwo* defined by hierarchical clustering versus CO_2 (**A–D**) and growth rate (**E–H**). Genes are plotted as solid lines and clusters are filled polygons, asterisk indicates gene clusters with significant Pearson correlation with CO_2 and dagger indicates a significant Pearson correlation with growth rate. Gene abbreviations: CA: carbonic anhydrase, Na^+/H^+: sodium/proton, SLC4: SLC4 family bicarbonate transporter, ALAT_GGAT: alanine amino transferase, psbO: photosystem II subunit O, sucB: 2-oxoglutarate dehydrogenase.

(Giordano et al. 2005; Raven 1997), however the localization of the gene product is unclear. The clustering analysis allows for discovery of genes that may be integral to a biophysical CCM that would be missed in a traditional targeted analysis. The putative regulatory genes also suggest how gene expression might be altered by CO_2-responsive signaling cascades similar to findings for diatoms (Harada et al. 2006; Hennon et al. 2015). The large multi-gene clusters (Fig. 4C, D) contain genes with many different functions with a few putative CCM genes, including the SLC4-2 bicarbonate

transporter (Fig. 4C, cluster 79) and three carbonic anhydrase genes, a bestrophin gene and a photorespiration gene (Fig. 4D, cluster 76). These clusters that were not significantly monotonically correlated with CO_2 (Supplementary Material Table S4), instead displaying a local maximum expression at ambient CO_2. Other genes in these clusters include genes associated with metabolism such as chlorophyll *a-b* binding and ATPase domains. The co-expression of these genes in *H. akashwio* suggests that these carbonic anhydrases and the bicarbonate transporter may be regulated by both metabolic and CO_2-responsive mechanisms, but disentangling these regulatory associations will require a greater number of experimental treatments than reported here.

Metabolic and regulatory genes formed clusters with significant correlations to growth rate (Fig. 4F,G,H and Supplementary Material Table S4). The photosystem II gene, *psbO*, was negatively correlated to growth rate (Pearson correlation = −0.56, *p*-value = 0.03, Fig. 4F), mirroring the results from the KEGG pathway analyses (Fig. 3). In contrast, the glycolysis and TCA cycle genes *sucB* and enolase were positively correlated with growth rate (Pearson correlation = 0.54, *p*-value = 0.04, Fig. 4G). These differences in gene expression reflect a variation in metabolic pathways underpinning and perhaps moderating the physiological response of *H. akashiwo* to changes in CO_2. Cluster 314 (Fig. 4H) contains gene transcription machinery with a significant anticorrelation to growth rate (Pearson correlation = −0.60, *p*-value = 0.02), suggesting that as growth rate increases there may be transcriptional changes. These gene clusters illustrate cell regulation and metabolic pathways that are influenced by CO_2 treatments, yet are intimately connected to growth and physiology of *H. akashiwo*.

To summarize the effect of future CO_2 scenarios on *H. akashiwo* gene expression and metabolism, the data were combined from KEGG pathways,

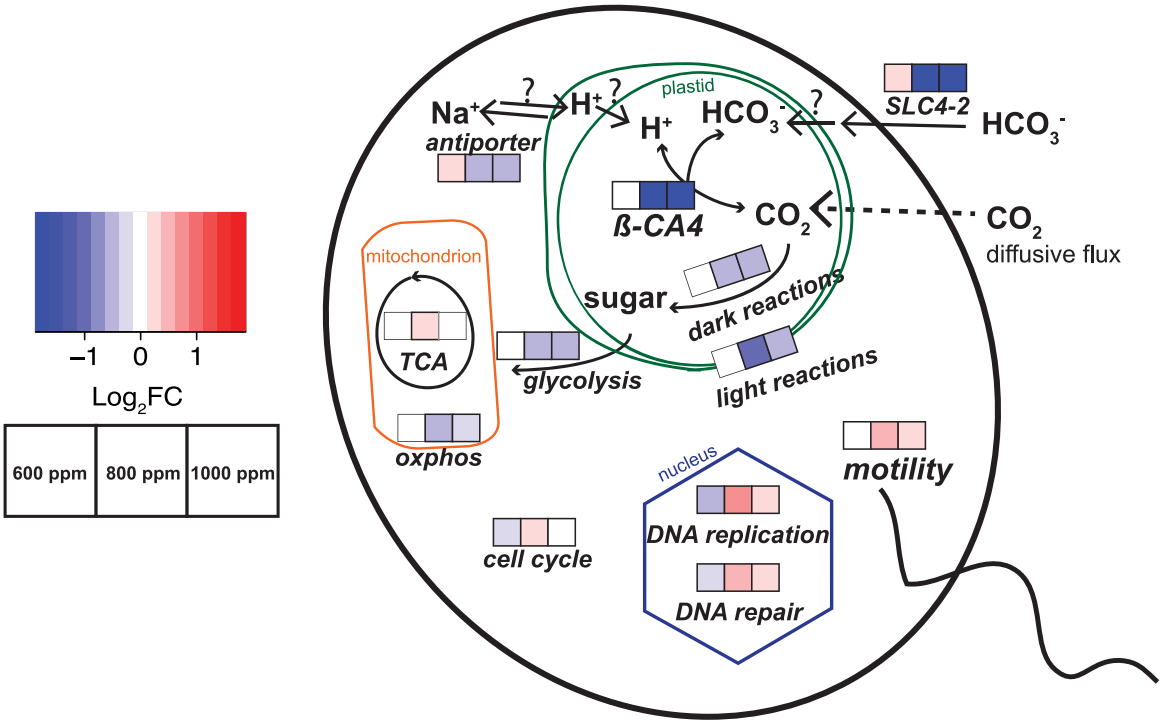

Figure 5. Summary of gene and metabolic pathway changes of *Heterosigma akashiwo* under three future CO_2 scenarios. The change in expression of genes, pathways, and gene clusters (bold italicized) are displayed as the log transformed Fold Change (log_2FC) compared to modern CO_2 for each projected future CO_2 treatment (600 ppm: left, 800 ppm: center, 1000 ppm: right). The reactions catalyzed by each gene product or pathway are represented by small arrows, transport with large arrows, and metabolites with bold text. The bolded wavy line represents a flagellum and the intracellular compartments are labeled as plastid (green), mitochondrion (orange), and nucleus (purple). Note that localizations of CCM gene products are putative (Table 2). Gene/pathway abbreviations: CA: carbonic anhydrase, SLC4: SLC4 family bicarbonate transporter, TCA: tricarboxylic acid cycle, oxphos: oxidative phosphorylation.

hierarchical clusters and single gene expression measurements (Fig. 5). The 600 ppm CO_2 treatment was similar to modern (~400 ppm) in gene expression. We hypothesize that the increase in CO_2 diffusive flux may not be enough to trigger the regulatory change in CCM genes and concurrent metabolic shifts. At 800 ppm CO_2, there was a marked decrease in expression of putative biophysical CCM genes (Fig. 5) consistent with the findings of Ji et al. (2018) for a *H. akashiwo* bloom and a decrease in most core metabolic pathways similar to the observations of decreased metabolic rates for the diatom *T. pseudonana* (Hennon et al. 2014, 2015). Cells grown in 800 ppm CO_2 had the fastest growth despite decreases in many core metabolic gene expression pathways such as the light and dark reactions of photosynthesis. One pathway that displayed the opposite trend at 800 ppm was the tricarboxylic acid cycle (TCA), which had increased expression. The gene expression of *H. akashiwo* at 800 ppm also suggests enhanced expression of cell cycle, DNA replication and DNA repair (Fig. 5). Elevated expression of motility genes was also seen at both 800 and 1000 ppm, which is consistent with previous observations of enhanced swimming behavior (Kim et al. 2013), but warrants further study. Cells grown at 1000 ppm displayed a similar decrease in biophysical CCM genes to 800 ppm (Fig. 5), yet with slower growth (Table 1, Fig. 1), potentially due to the inhibitory effects of acidification. Cells grown at 1000 ppm also had weaker increases in cell cycle, DNA replication and repair and no increase in the TCA cycle. These gene expression changes indicate a non-linear response to elevated CO_2 with potential thresholds around different future emissions scenarios, mirroring the non-linear growth response of *H. akashiwo* to CO_2. These genetic changes from *H. akashiwo* integrate the alga's responses to the CO_2 treatment as well as any shifts in the co-cultured bacterial community due to CO_2 which have been shown to be significant (Bunse et al. 2016; Hennon et al. 2018). This study therefore represents a holistic view of how this harmful alga responds to rising CO_2 as part of the microbial community. These genetic responses demonstrate the complexity underlying the mechanisms driving phytoplankton responses to future CO_2 and point to differences in future HAB risk that are dependent on CO_2 concentration pathways.

Conclusions

Although single condition studies that focus on phytoplankton responses to ambient versus elevated CO_2 are increasingly common (e.g.: Fu et al. 2008; Hennon et al. 2017), there are fewer studies that identify responses over a range of future CO_2 concentration scenarios. Here we identified an optimum CO_2 concentration for *H. akashiwo* growth around 600–800 ppm. This new functional response curve for *H. akashiwo* could be used in numerical models to improve HAB prediction, and such response curves along with estimates of evolutionary potential will be critical for accurately parameterizing models of future ocean phytoplankton biogeography. The gene expression changes support the observation of a shift in cell state between 600 and 800 ppm with a decrease in many core metabolic pathways and an increase in cell cycle and DNA replication pathways. Of the dozens of putative CCM genes in *H. akashiwo*, three beta-CAs and a few other CCM genes were significantly negatively correlated with CO_2, suggesting that these genes may be central to the response of this raphidophyte to changes in CO_2. Motility genes were also significantly correlated with CO_2 concentration, which may drive changes in swimming behavior at elevated CO_2. This work highlights the potential of whole transcriptome data for elucidating mechanisms of environmental response in ecologically important species such as *H. akashiwo*. Moving forward, the use of a range of treatments is essential to uncover non-linear responses in physiology and gene expression where processes such as CO_2 limitation and inhibition may be occurring simultaneously and where there may be environmental thresholds for gene activation and suppression.

Methods

Cultures and acclimation: Unialgal, non-axenic cultures of *Heterosigma akashiwo* (CCMP2393) were grown in L1 medium (without silicate) made with a Long Island Sound seawater base collected from Avery Point, CT, USA (salinity 32) at 18 °C with a 14:10 (light:dark) cycle with an irradiance of approximately 100 μmol m^{-2} s^{-1}. Cells were acclimated in exponential growth phase to different carbonate chemistries in 1.2 L of L1 media in 2.5-L polycarbonate bottles. To control the carbonate chemistry of the water, the headspace of each bottle was purged continuously with a custom gas mixture of ~21% oxygen, ~79% nitrogen and either 200, 400, 600, 800 or 1000 ppmv CO_2 (TechAir, NY). The gas streams were pre-filtered through 0.2-μm HEPA filters and directed through a sterile glass pipette to break the boundary layer of the media without contacting the surface. The bottles were not bubbled to avoid the adverse effects of turbulence on phytoplankton growth (Juhl and Latz 2002; Thomas and Gibson 1990). The bottles were rotated gently (80 rpm) on an orbital shaker during acclimation. The headspace of each bottle was purged for at least one day prior to inoculation and continuously during the acclimation. Cells

were acclimated for three days in each of the five CO_2 concentrations prior to the start of the experiment. Cell concentrations were kept below $\sim 10^5$ cells mL^{-1}, as estimated by relative fluorescence, to prevent alteration of carbonate chemistry.

CO_2 growth rate experiment: After acclimation, approximately 5×10^4 cells in ~100 mL were transferred to triplicate 2.5-L bottles with 1.2 L of L1 media that had been purged with the same gas mixture as described above for a starting concentration of ~200–400 cells mL^{-1} determined by cell counts. At approximately the same time each day, each culture was thoroughly mixed and sub-sampled for cell counts, relative fluorescence, and pH. During the experiment, growth was monitored by relative fluorescence using an AquaFlash handheld fluorometer (Turner Designs, San Jose, CA). At the end of the experiment, growth calculations were derived from cell counts. For cell counts, 1 mL of each triplicate culture was preserved in 2% Lugol's solution (final concentration) at room temperature and counted within a month of preservation under a microscope. Growth rates were calculated from the slope of the natural log of cell concentration versus time and fit to all time points (Supplementary Material Fig. S1). The exception to this was for one replicate from each of the CO_2 treatments for 800 and 1000 ppm, where only the last four points were used due to evidence of an initial lag phase. The natural log of cell concentration increased linearly over time with $R^2 > 0.93$ for all replicates (Supplementary Material Fig. S1). pH was tracked using the method described below. After five days, the cultures reached the target concentration of $\sim 10^4$ cells mL^{-1}, determined by preliminary experiments to have negligible impact on the carbonate chemistry, and were harvested for RNA sequencing, hydrogen peroxide concentration, *in vitro* chlorophyll concentration, and elemental composition.

Carbonate chemistry measurements: During the experiment, daily samples were collected and pH was measured using the m-cresol purple method (Dickson et al. 2007) at 25 °C using a Shimadzu UV-1800 spectrophotometer (Kyoto, Japan). Samples for total alkalinity were collected at the start and end of each experiment and measured with the closed-cell titration method (Dickson et al. 2007). Briefly, about 180 mL of culture or sterile media was collected in a glass bottle with a ground glass stopper and poisoned with 20 μL of saturated mercuric chloride solution and stored at room temperature for up to two weeks before analysis. Approximately 100 mL of each sample was run on a Metrohm Titrando titrator (Herisau, Switzerland), calibrated with certified reference materials from the Dickson lab (Scripps Institution of Oceanography, La Jolla, CA). The total alkalinity and pH measurements were then used to calculate the daily CO_2 concentration in the media using CO2Calc software (Lewis and Wallace 1998). Due to variability in the aqueous CO_2 concentrations within some replicate bottles over the five days of the experiment, replicates were discarded from further analysis if the standard deviation of pCO_2 within a bottle exceeded 90 ppm over the course of the experiment. The replicates that met quality control thresholds were analyzed from two separate runs to include three biological replicates per CO_2 treatment, totaling fifteen experimental replicates (Supplementary Material Table S1).

Physiology and elemental analysis: At the time of harvest, samples were collected for chlorophyll *a*, elemental composition, and hydrogen peroxide concentration. For chlorophyll *a*, 150 mL ($\sim 6 \times 10^6$ cells) was filtered on to a 5 μm polycarbonate filter (25 mm). Chlorophyll *a* concentration was determined according to Strickland and Parsons (1972). Briefly, the samples were extracted in 10 mL of 90% methanol, vortexed for 15 s, and stored in the dark at −20 °C for 12 h. The fluorescence in the supernatant was then measured on a Turner Designs Aquafluor fluorometer before and after acidification with 0.1N hydrochloric acid. The fluorometer was calibrated with chlorophyll *a* from *Anacystis nidulans* (Sigma). For elemental composition (POC and PON), 150 mL ($\sim 6 \times 10^6$ cells) was filtered on to duplicate pre-combusted glass fiber (GF/F) 25 mm filters, and stored in pre-combusted foil. Filters were stored at −80 °C until analysis. Prior to analysis, filters were dried at 60 °C for 12 hours, weighed and quartered. Elemental analyses were performed using a Costech ECS4010 elemental analyzer EA (Costech Analytical Technologies Inc., Valencia, CA), interfaced with ConFlo IV and Thermo Delta V plus mass spectrometer, and calibrated by acetanilide. To correct for the carbon content of a clean, combusted GF/F filter, 7.35 μg (the mean C content of two blanks) was subtracted from the C value of each sample. For hydrogen peroxide concentration, 1 mL of each replicate culture was transferred to a snap-cap tube, stored in the dark at room temperature, and analyzed within 3 hours. Samples were measured using the Amplex Red Hydrogen Peroxide/Peroxidase Assay Kit (ThermoFisher Scientific, Waltham, MA). H_2O_2 concentrations were normalized per cell for each replicate culture.

RNA extraction and sequencing: At the point of harvest, 150 mL ($\sim 6 \times 10^6$ cells) were filtered on to 5 μm pore size, 25 mm polycarbonate filter and flash frozen in liquid nitrogen. Genetic material from samples was extracted with the RNeasy Mini kit (Qiagen, Valencia, CA) and DNA was removed on-column using the RNase-free DNase Set (Qiagen), yielding total RNA. Total RNA extracts of the triplicate cultures were quantified on a 2100 Bioanalyzer (Agilent, Santa Clara, CA). Libraries were prepared using poly-A pull down with the TruSeq Stranded mRNA Library Prep kit (Illumina, San Diego, CA). This pull down step precluded a joint analysis of bacterial responses, but allowed for more targeted sequencing to track *H. akashiwo* responses. Library preparation, barcoding, and sequencing from each library was performed by the JP Sulzberger Columbia University Genome Center (New York, NY). Samples were sequenced on an Illumina HiSeq 2500 to a depth of 60 million paired-end reads (2×100 bp). The sequencing data are archived with NCBI (BioProject: PRJNA377729, SRA: SRX4737278-SRX4737292). Reads were aligned using Bowtie2 (Langmead and Salzberg 2012) to the MMETSP consensus contigs for *Heterosigma akashiwo* CCMP2393 (https://omictools.com/marine-microbial-eukaryotic-transcriptome-sequencing-project-tool). Relative gene expression patterns were determined by tabulating read counts for each contig, normalizing for differences in sequencing effort, and calculating the fold change in expression with the biological variation of the replicates described in the *Statistics* section below and in McCarthy et al. (2012). While these expression patterns were not independently validated with an alternative approach like qRT-PCR, previous work with other algae has established that similar analytical pipelines have reconstructed independently verified expression patterns (Dyhrman et al. 2012; Wurch et al. 2011).

Statistics: Exponential growth rates from this study and from other available studies with *H. akashiwo* measured under ~200–1000 ppm CO_2 (Bianco et al. 2016; Fu et al. 2008; Hennon et al. 2017; Kim et al. 2013; Stewart et al. 2015) were fit with a modified CO_2 limitation-inhibition model (Equation (1)) modified from Bach et al. (2015).

$$\mu = \frac{a * CO_2}{b + CO_2} - e^{(c * CO_2)} \quad (1)$$

Where growth rate (μ) is a function of the Monod-limitation by CO_2 with the maximum growth rate (a) and half-saturation of growth with CO_2 (b) and the inhibition of growth by high CO_2 (c). The best fit was calculated using the non-linear least

squares function (nls, R) with starting guesses: a = 1, b = 100, $c = 1 \times 10^{-5}$. To calculate a standard deviation envelope for the model fit, uncertainties were propagated by the Monte Carlo method, wherein the non-linear model was fit in 1000 simulations by drawing each point randomly from a Gaussian distribution with the standard deviation reported for the uncertainty in growth rate and CO_2 concentration.

Significant differences between physiological parameters by CO_2 treatment were assessed with analysis of variance (ANOVA) and Tukey's honestly significant differences test (aov and TukeyHSD, stats, R). Differential expression of genes in any CO_2 treatment compared to modern was determined using the general linear model (GLM) exact test (edgeR, R). Briefly, the read counts were normalized by trimmed mean of M-values (TMM) using the function calcNormFactors, tagwise dispersions were calculated with the function estimateGLMTagwiseDisp, a GLM was fit using glmFit, and $\log_2$ fold change (logFC) for each treatment was calculated relative to average expression at modern CO_2. *P*-values from likelihood ratio tests were corrected for multiple testing using the false discovery method (fdr). To measure changes in whole pathway expression, genes were annotated by Kyoto encyclopedia of genes and genomes (KEGG) ID with the online tool GhostKOALA (Kanehisa et al. 2016) and differences in distributions of KEGG pathway gene expression relative to 400 ppm CO_2 were assessed with a Kolmogorov-Smirnov test (ks.test, stats, R). The predicted localization of genes products were determined by SignalP (http://www.cbs.dtu.dk/services/SignalP/) version 4.1 and ASAFind (http://rocaplab.ocean.washington.edu/tools/asafind/) with default confidence thresholds. To characterize genes of unknown function and determine co-expression patterns of genes, the genes were hierarchically clustered (hclust, fastcluster, R) based on Pearson distance (pearson.dist, hyperSpec, R), and cut at an arbitrary height to yield 500 clusters (cutree, stats, R). Individual genes and gene clusters were tested for significant correlations to both CO_2 concentrations and growth rate using the Pearson test (cor.test, stats, R).

Contributions: GMMH, STH, and STD designed the study, GMMH and OMW performed the experiments, OMW and MDHL performed laboratory analyses, GMMH performed RNA extractions, GMMH, OMW and MDHL performed computational analysis, GMMH wrote the manuscript with contributions from all authors.

Acknowledgements

This work was supported by the National Science Foundation Biological Oceanography Program #OCE1314336 (STD), with partial support also provided by WSL Pure in partnership with Columbia University's Center for Climate and Life, the Paul M. Angell Family Foundation, Columbia Earth Institute Research Assistantship (OMW), and The Columbia University Bridge to PhD Program in the Natural Sciences Research Assistantship (MDHL). We thank Hugh Ducklow and Naomi Shelton for the use of and training on the autotitrator and Andrew Juhl for contributions to the original experimental design and construction of a CO_2 flowmeter manifold.

Appendix A. Supplementary Data

Supplementary data associated with this article can be found, in the online version, at https://doi.org/10.1016/j.protis.2018.10.002.

References

Anderson DM, Cembella AD, Hallegraeff GM (2012) Progress in understanding harmful algal blooms: paradigm shifts and new technologies for research, monitoring, and management. Annu Rev Mar Sci **4**:143–176

Bach LT, Riebesell U, Gutowska MA, Federwisch L, Schulz KG (2015) A unifying concept of coccolithophore sensitivity to changing carbonate chemistry embedded in an ecological framework. Prog Oceanogr **135**:125–138

Bearon RN, Grunbaum D, Cattolico RA (2004) Relating cell-level swimming behaviors to vertical population distributions in *Heterosigma akashiwo* (Raphidophyceae), a harmful alga. Limnol Oceanogr **49**:607–613

Bianco CM, Stewart JJ, Miller KR, Fitzgerald C, Coyne KJ (2016) Light intensity impacts the production of biofuel intermediates in *Heterosigma akashiwo* growing on simulated flue gas containing carbon dioxide and nitric oxide. Bioresour Technol **219**:246–251

Brierley AS, Kingsford MJ (2009) Impacts of climate change on marine organisms and ecosystems. Curr Biol **19**:R602–R614

Bunse C, Lundin D, Karlsson CMG, Vila-Costa M, Palovaara J, Akram N, Svensson L, Holmfeldt K, González JM, Calvo E, Pelejero C, Marrasé C, Dopson M, Gasol JM, Pinhassi J (2016) Response of marine bacterioplankton pH homeostasis gene expression to elevated CO_2. Nat Climate Change **6**:1–7

Butrón A, Madariaga I, Orive E (2012) Tolerance to high irradiance levels as a determinant of the bloom-forming *Heterosigma akashiwo* success in estuarine waters in summer. Estuar Coast Shelf Sci **107**:141–149

Caldeira K, Wickett ME (2003) Anthropogenic carbon and ocean pH. Nature **425**:365

Ciais P, Sabine C, Bala G, Bopp L, Brovkin V, Canadell J, Chhabra A, DeFries R, Galloway J, Heimann M, Jones C, Le Quéré C, Myneni R.B, Piao S, Thornton P (2013) Carbon and Other Biogeochemical Cycles. In Climate Change 2013: The Physical Science Basis. Contribution of Working Group I to the Fifth Assessment Report of the Intergovernmental Panel on Climate Change [Stocker, T.F., D. Qin, G.-K. Plattner, M., Tignor, S.K., Allen, J., Boschung, A., Nauels, Y., Xia, V. Bex and P.M. Midgley (eds.)]. Available from www.climatechange2013.org and www.ipcc.ch

Daley J (2018) Toxic algae closes important Maine shellfish region. Smithsonian.com

Descolas-Gros C, Oriol L (1992) Variations in carboxylase activity in marine phytoplankton cultures. B-carboxylation in carbon flux studies. Mar Ecol Prog Ser **85**:163–169

Dickson AG, Sabine CL, Christian JR (eds) Guide to Best Practices for Ocean CO_2 Measurements. PICES Spec Publ

3. North Pacific Marine Science Organization Sidney, British Columbia, 191 p

Doney SC, Fabry VJ, Feely RA, Kleypas JA (2009) Ocean acidification: the other CO_2 problem. Annu Rev Mar Sci **1**:169–192

Dorantes-Aranda JJ, Seger A, Mardones JI, Nichols PD, Hallegraeff GM (2015) Progress in understanding algal bloom-mediated fish kills: The role of superoxide radicals, phycotoxins and fatty acids. PLoS ONE **10(7)**:e0133549

Dutkiewicz S, Morris JJ, Follows MJ, Scott J, Levitan O, Dyhrman ST, Berman-Frank I (2015) Impact of ocean acidification on the structure of future phytoplankton communities. Nat Climate Chang **5**:1002–1006

Dyhrman ST, Jenkins BD, Rynearson TA, Saito MA, Mercier ML, Alexander H, Whitney LAP, Drzewianowski A, Bulygin VV, Bertrand EM, Wu Z, Benitez-Nelson C, Heithoff A (2012) The transcriptome and proteome of the diatom *Thalassiosira pseudonana* reveal a diverse phosphorus stress response. PLoS ONE **7(3)**:e33768

Feely RA, Alin SR, Newton J, Sabine CL, Warner M, Devol A, Krembs C, Maloy C (2010) The combined effects of ocean acidification, mixing, and respiration on pH and carbonate saturation in an urbanized estuary. Estuar Coast Shelf Sci **88**:442–449

Fu FX, Zhang Y, Warner ME, Feng Y, Sun J, Hutchins DA (2008) A comparison of future increased CO_2 and temperature effects on sympatric Heterosigma akashiwo and Prorocentrum minimum. Harmful Algae **7**:76–90

Giordano M, Beardall J, Raven JA (2005) CO_2 concentrating mechanisms in algae: mechanisms, environmental modulation, and evolution. Annu Rev Plant Biol **56**: 99–131

Gobler CJ, Doherty OM, Hattenrath-Lehmann TK, Griffith AW, Kang Y, Litaker RW (2017) Ocean warming since 1982 has expanded the niche of toxic algal blooms in the North Atlantic and North Pacific oceans. Proc Natl Acad Sci USA **114**:4975–4980

Haley ST, Alexander H, Juhl AR, Dyhrman ST (2017) Transcriptional response of the harmful raphidophyte *Heterosigma akashiwo* to nitrate and phosphate stress. Harmful Algae **68**:258–270

Hallegraeff GM (1993) A review of harmful algal blooms and their apparent global increase. Phycologia **32**:79–99

Hallegraeff GM (2010) Ocean climate change, phytoplankton community responses, and harmful algal blooms: a formidable predictive challenge. J Phycol **46**:220–235

Harada H, Nakajima K, Sakaue K, Matsuda Y (2006) CO_2 sensing at ocean surface mediated by cAMP in a marine diatom. Plant Physiol **142**:1318–1328

Hennon GMM, Hernández Limón MD, Haley ST, Juhl AR, Dyhrman ST (2017) Diverse CO_2-induced responses in physiology and gene expression among eukaryotic phytoplankton. Front Microbiol **8**:2547

Hennon GMM, Quay P, Morales RL, Swanson LM, Armbrust EV (2014) Acclimation conditions modify physiological response of the diatom *Thalassiosira pseudonana* to elevated CO_2 concentrations in a nitrate-limited chemostat. J Phycol **50**:243–253

Hennon GMM, Ashworth J, Groussman RD, Berthiaume C, Morales RL, Baliga NS, Orellana MV, Armbrust EV (2015) Diatom acclimation to elevated CO_2 via cAMP signalling and coordinated gene expression. Nat Climate Chang **5**:761–766

Hennon GMM, Morris JJ, Haley ST, Zinser ER, Durrant A, Entwistle E, Dokland T, Dyhrman ST (2018) The impact of elevated CO_2 on *Prochlorococcus* and microbial interactions with helper bacterium *Alteromonas*. ISME J **12**:520–531

Honjo T. (1992) Harmful Red Tides of *Heterosigma akashiwo*. In Svrjecek RS (ed) Control of Disease in Aquaculture. NOAA Technical Report NMFS 111, pp 27–32

Itakura S, Imai I. (2014) Economic Impacts of Harmful Algal Blooms on Fisheries and Aquaculture in Western Japan- An Overview of Interannual Variability and Interspecies Comparison. In Trainer VL, Yoshida T (eds) Proceedings of the Workshop on Economic Impacts of Harmful Algal Blooms on Fisheries and Aquaculture, PICES Sci Rep No 47, pp 17–26

Ji N, Lin L, Li L, Yu L, Zhang Y, Luo H, Li M, Shi X, Wang Da-Zhi, Lin S (2018) Metatranscriptome analysis reveals environmental and diel regulation of *Heterosigma akashiwo* (*Raphidophyceae*) bloom. Environ Microbiol **20**:1078–1094

Juhl AR, Latz MI (2002) Mechanisms of fluid shear-induced inhibition of population growth in a red-tide dinoflagellate. J Phycol **38**:683–694

Kanehisa M, Sato Y, Morishima K (2016) BlastKOALA and GhostKOALA: KEGG tools for functional characterization of genome and metagenome sequences. J Mol Biol **428**:726–731

Keeling PJ, Burki F, Wilcox HM, Allam B, Allen EE, Amaral-Zettler LA, Armbrust EV, et al. (2014) The marine microbial eukaryote transcriptome sequencing project (MMETSP): illuminating the functional diversity of eukaryotic life in the oceans through transcriptome sequencing. PLoS Biol **12(6)**:e1001889

Kim H, Spivack AJ, Menden-Deuer S (2013) pH alters the swimming behaviors of the raphidophyte *Heterosigma akashiwo*: implications for bloom formation in an acidified ocean. Harmful Algae **26**:1–11

Langmead B, Salzberg SL (2012) Fast gapped-read alignment with Bowtie 2. Nat Meth **9**:357–360

Lewis E, Wallace D (1998) Program Developed for CO_2 System Calculations. US DOE Environmental Sciences Division publication number 4735

McCarthy DJ, Chen Y, Smyth GK (2012) Differential expression analysis of multifactor RNA-Seq experiments with respect to biological variation. Nucleic Acids Res **40**:4288–4297

Nakajima K, Tanaka A, Matsuda Y (2013) SLC4 family transporters in a marine diatom directly pump bicarbonate from seawater. Proc Natl Acad Sci USA **110**:1767–1772

Nimer NA, Iglesias-Rodriguez MD, Merrett MJ (1997) Bicarbonate utilization by marine phytoplankton species. J Phycol **33**:625–631

Ou G, Wang H, Si R, Guan W (2017) The dinoflagellate *Akashiwo sanguinea* will benefit from future climate change: the interactive effects of ocean acidification, warming and high irradiance on photophysiology and hemolytic activity. Harmful Algae **68**:118–227

Pang M, Xu J, Qu P, Mao X, Wu Z, Xin M, Sun P, Wang Z, Zhang X, Chen H (2017) Effect of CO_2 on growth and toxicity of

Alexandrium tamarense from the East China Sea, a major producer of paralytic shellfish toxins. Harmful Algae **68**:240–247

Raven J (1997) CO_2-concentrating mechanisms: a direct role for thylakoid lumen acidification? Plant Cell Environ **20**:147–154

Rensel JEJ, Haigh N, Tynan TJ (2010) Fraser river sockeye salmon marine survival decline and harmful blooms of *Heterosigma akashiwo*. Harmful Algae **10**:98–115

Riebesell U, Schulz KG, Bellerby RGJ, Botros M, Fritsche P, Meyerhöfer M, Neill C, Nondal G, Oschlies A, Wohlers J, Zöllner E (2007) Enhanced biological carbon consumption in a high CO_2 ocean. Nature **450**:545–548

Sabine CL, Feely R, Gruber N, Key RM, Lee K, Bullister JL, Wanninkhof R, Wong CS, Wallace DWR, Tilbrook B, Millero FJ, Peng Tsung-Hung, Kozyr A, Ono T, Rios AF (2004) The oceanic sink for anthropogenic CO_2. Science **305**:367–371

Stewart JJ, Bianco CM, Miller KR, Coyne KJ (2015) The marine microalga, *Heterosigma akashiwo*, converts industrial waste gases into valuable biomass. Front Energy Res **3**:12

Strickland JDH, Parsons TR (1972) Pigment Analysis. A Practical Handbook of Seawater Analysis. 2nd ed. Fisheries Research Board of Canada, Ottawa Canada, pp 201–203

Strom SL, Harvey EL, Fredrickson KA, Menden-Deuer S (2013) Broad salinity tolerance as a refuge from predation in the harmful raphidophyte alga *Heterosigma akashiwo* (*Raphidophyceae*). J Phycol **49**:20–31

Taylor FJR, Haigh R (1993) The Ecology of Fish-killing Blooms of the Chloromonad Flagellate *Heterosigma* in the Strait of Georgia and Adjacent Waters. In Smayda TJ, Shimizu Y (eds) Toxic Phytoplankton Blooms in the Sea. Elsevier Science Publishers, pp 705–710

Thomas WH, Gibson CH (1990) Effects of small-scale turbulence on microalgae. J Appl Phycol **2**:71–77

Twiner MJ, Trick CG (2000) Possible physiological mechanisms for production of hydrogen peroxide by the ichthyotoxic flagellate *Heterosigma akashiwo*. J Plankton Res **22**:1961–1975

Twiner MJ, Dixon SJ, Trick CG (2001) Toxic effects of *Heterosigma akashiwo* do not appear to be mediated by hydrogen peroxide. Limnol Oceanogr **46**:1400–1405

Wurch LL, Bertrand EM, Saito MA, Van Mooy BAS, Dyhrman ST (2011) Proteome changes driven by phosphorus deficiency and recovery in the brown tide-forming alga *Aureococcus anophagefferens*. PLoS ONE **6(12)**:e28949

Xu D, Zhou B, Wang Y, Ju Q, Yu Q, Tang X (2010) Effect of CO_2 enrichment on competition between *Skeletonema costatum* and *Heterosigma akashiwo*. Chinese J Oceanol Limnol **28**:933–939

Zhang Y, Fu FX, Whereat E, Coyne KJ, Hutchins DA (2006) Bottom-up controls on a mixed-species HAB assemblage: A comparison of sympatric *Chattonella subsalsa* and *Heterosigma akashiwo* (*Raphidophyceae*) isolates from the Delaware Inland Bays, USA. Harmful Algae **5**:310–320

Available online at www.sciencedirect.com

ScienceDirect